



Loess and other quaternary sediments in Germany

Frank Lehmkuhl, Stephan Pötter, Annika Pauligk & Janina Bösken

To cite this article: Frank Lehmkuhl, Stephan Pötter, Annika Pauligk & Janina Bösken (2018) Loess and other quaternary sediments in Germany, Journal of Maps, 14:2, 330-340, DOI: [10.1080/17445647.2018.1473817](https://doi.org/10.1080/17445647.2018.1473817)

To link to this article: <https://doi.org/10.1080/17445647.2018.1473817>



© 2018 The Author(s). Published by Informa UK Limited, trading as Taylor & Francis Group on behalf of journal of Maps



[View supplementary material](#)



Published online: 21 May 2018.



[Submit your article to this journal](#)



[View related articles](#)



[View Crossmark data](#)



Loess and other quaternary sediments in Germany

Frank Lehmkuhl , Stephan Pötter , Annika Pauligk and Janina Bösken

Department of Geography, RWTH Aachen University, Aachen, Germany

ABSTRACT

Geo- and palaeoecological studies focusing on the late Pleistocene require a detailed knowledge of the spatial distribution of aeolian sediments. In Germany, existing maps are either on large scales, have a regional focus or show significant inaccuracies such as artificial boundaries within different geological units. To obtain a more detailed, seamless map of the distribution of aeolian sediments and their potential source areas, we combined and reanalysed available geodata, using a Geographical Information System. The resultant maps (scale: approx. 1:2,600,000) show the link between source areas and the late Quaternary aeolian deposits in Germany and can provide one context for further work on, e.g. palaeogeographical studies. This work was compared with other already published datasets and the problems of sediment mapping at a small scale were discussed.

ARTICLE HISTORY

Received 22 March 2018
Revised 2 May 2018
Accepted 3 May 2018

KEYWORDS

Aeolian sediments; dust sources; spatial data; GIS; central Europe

1. Introduction

The deposition of aeolian sediments depends on specific geographic conditions (Pécsi, 1990, 1991). Four factors are required for the formation of aeolian sediment bodies: (1) a dust source, from which the sediment is deflated, (2) sufficient wind energy, (3) a sink, where the topographic and environmental conditions favour the sediment deposition and (4) a sufficiently long period of time (Pye, 1995; Smalley, Marković, & Svirčev, 2011). Since loess in Europe was mainly accumulated during the cold stages of the Quaternary (Marković et al., 2015; Muhs & Bettis, 2003), the distribution pattern of aeolian sediments and their potential source areas give important information about palaeogeographical conditions (Sprafke & Obrecht, 2016). Moreover, the relevance of loess is manifold: the world's most fertile soils are developed in loess (Catt, 1988, 2001; Pécsi & Richter, 1996; Smalley, Jefferson, Dijkstra, & Derbyshire, 2001); and well-preserved Palaeolithic and Neolithic artefacts can be found in loess or loess-like sediments (Antoine, Catt, Lautridou, & Sommé, 2003; Einwögerer et al., 2006; Gerlach, Baumewerd-Schmidt, van den Borg, Eckmeier, & Schmidt, 2006; Händel, Simon, Einwögerer, & Neugebauer-Maresch, 2009; Neugebauer-Maresch, Einwögerer, Richter, Maier, & Hussain, 2016; Pécsi & Richter, 1996; Rensink, 2010; Tasić, Penezić, Marković, & Catto, 2017; Terhorst et al., 2013).

'Loess maps' have a long history in Quaternary science. Grahmann (1932) developed the first map of loess distribution in central Europe, which was adapted and compiled with source areas by Flint (1971). Fink,

Haase, and Ruske (1977) created a map for Western, Central and Eastern Europe at a scale of 1:2,500,000 in collaboration with researchers from various countries. This map was completed and digitised by Haase et al. (2007). Other maps published in scientific studies during the last decades are characterised by either a regional (Antoine et al., 2003; Lill & Smalley, 1978) or a global scale (Muhs & Bettis, 2003; Pécsi, 1990).

Maps at a small scale often lack accuracy or show inconsistencies such as artificial breaks at administrative boundaries. This is related to different terminological and methodological foci of the contributors (Haase et al., 2007). Most researchers accept these problems, so that the map according to Haase et al. (2007) is widely accepted in Quaternary science. Recently, however, there were some attempts to create more precise maps of loess distribution. For instance, Lindner, Lehmkuhl, and Zeeden (2017) used paedological information to fill gaps in the Haase map in western Romania. Bertran, Liard, Sitzia, and Tissoux (2016) used topsoil textural data from the Land Use and Cover Area frame Statistical survey database (LUCAS, Orgiazzi, Ballabio, Panagos, Jones, & Fernández-Ugalde, 2018; Tóth, Jones, & Montanarella, 2013) to create a map of aeolian sediments in Europe, with a focus on France.

To follow-up on the recent research, both methodologically and geographically, the aim of this study is the creation of a detailed, seamless map of the distribution of aeolian sediments and their potential source areas in Germany. In further studies, these maps could be used

for palaeolandscape modelling. For these objectives, we reanalysed and combined free, online available data of the Federal Institute for Geoscience and Natural Resources of Germany (Bundesanstalt für Geowissenschaften und Rohstoffe, BGR), to get a detailed overview of the distribution of aeolian sediments within Germany.

2. Study area

Germany is located in Central Europe and according to [Liedtke and Marcinek \(2002\)](#) it can be divided into five main parts: (a) the north German lowlands, which are dominated by a low relief formed by Pleistocene glacial and periglacial processes; (b) the central part with mountains composed of folded Palaeozoic rocks and

partly covering sedimentary bedrock; (c) the south German scarplands, which are dominated by cuestas of sedimentary bedrock; (d) the Tertiary molasse sediment basin including remnants of piedmont glaciations south of the Danube River and in the foreland of the Alps; and (e) the Alps with their high mountain environment in the south.

Regarding its geography, the loess distribution in Germany follows a specific pattern, which allows the division in four main loess regions (cf. [Lehmkuhl, Zens, Krauß, Schulte, & Kels, 2016](#)) (Figure 1):

- (1) The northern Central European loess belt between the former ice marginal position of the Weichselian ice sheet in the north and the German uplands (e.g. Rhenish shield, Harz Mountains and Ore

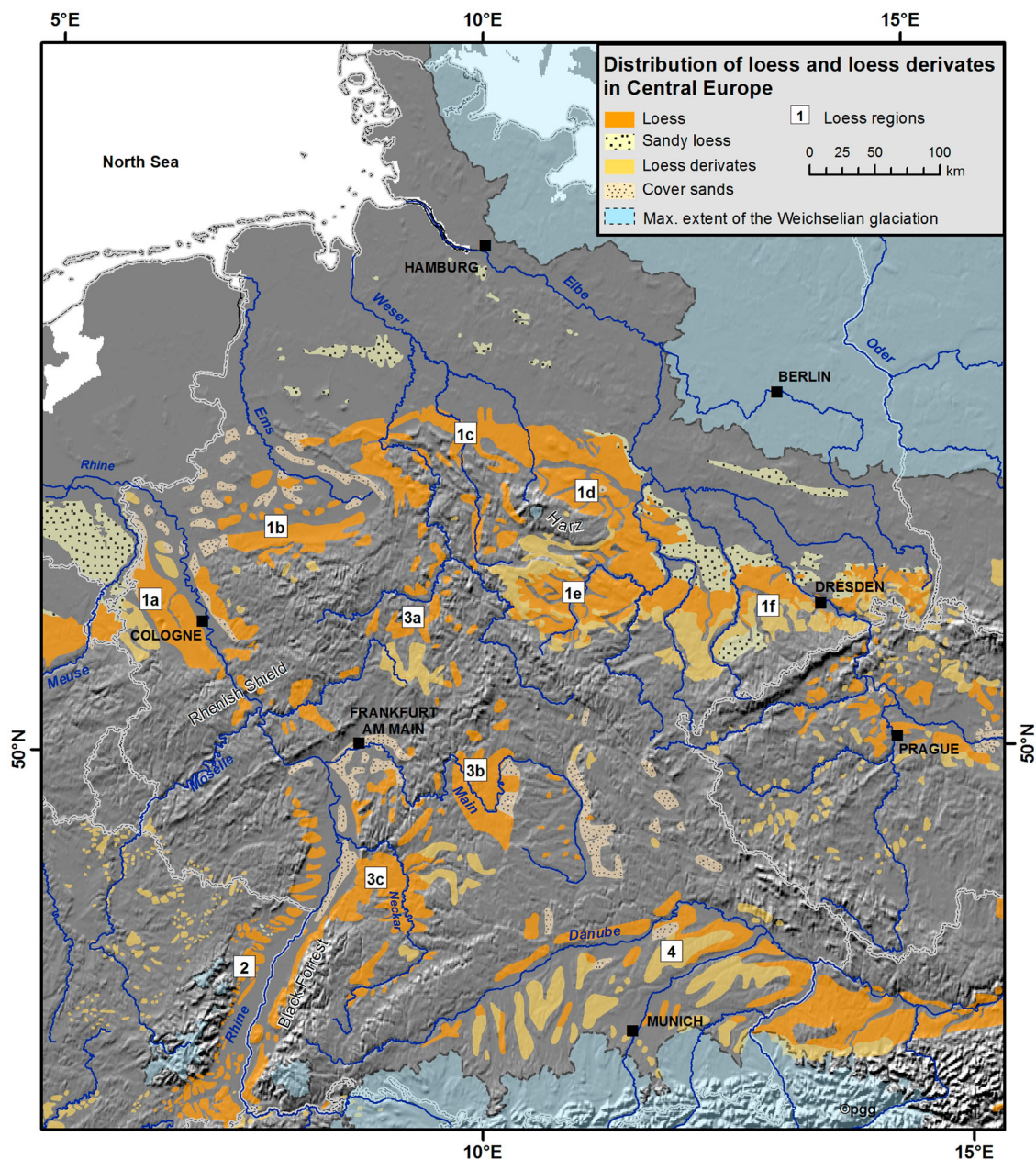


Figure 1. Study area, modified according to [Lehmkuhl et al. \(2016\)](#). The distribution of aeolian sediments is according to [Haase et al. \(2007\)](#). The numbers refer to the main loess regions and the letters to the subregions listed in the text. Ice extent modified according to [Ehlers, Eissmann, Lippstreu, Stephan, and Wansa \(2004\)](#) and [Ehlers, Grube, Stephan, and Wansa \(2011\)](#).

- Mountains) in the south. [Lehmkuhl et al. \(2016\)](#) subdivided this region into six subregions: (1a) the Lower Rhine Embayment; (1b) the southern part of Westphalia, including the Westphalian Lowlands and the Soest Börde; (1c) the southern parts of Lower Saxony including Hildesheim Börde; (1d) Saxony-Anhalt including the foreland of the Harz Mountains; (1e) the basins of Thuringia and (1f) loess regions in Saxony.
- (2) The Upper Rhine Valley (Upper Rhine Graben) including the Mainz basin at the southernmost margin of the Rhenish shield.
 - (3) The basins of the German uplands in central and southwestern Germany. These can be subdivided into: (3a) the basins in Lower Saxony and Hesse; (3b) the basins in Franconia and (3c) the Kraichgau area.
 - (4) Along the German stretches of the Danube River, mainly in the southern part of Bavaria.

3. Methods and data sources

3.1. Source maps, spatial data and processing

The presented maps build upon freely available data from the BGR. For the mapping of the potential source areas of aeolian deposits, the digital geological map of Germany with a scale of 1:1,000,000 was used ([Toloczyki, Trurnit, Voges, Wittekind, & Zitzmann, 2006](#)). Even though a dataset with a larger scale would be more precise, the nomenclature of those maps was too differentiated to be integrated into the present map. Therefore, we used this map, in order of generalisation.

Generally considered dust source areas for loess deposits are the shelves of the North Sea and the English Channel ([Antoine et al., 2013](#)) and late Pleistocene accumulations of fluvial origin, including the areas covered by Holocene fills today that were part of the Pleistocene braided river systems ([Smalley et al., 2009](#)). In addition, the last glacial outwash-plains and fluvio-glacial valleys (German: Urstromtäler) are considered as dust source areas ([Bertran et al., 2016](#); [Smalley et al., 2009](#)). These different units were extracted from the attribute table of the geological map ([Toloczyki et al., 2006](#)) and are shown in map A (Main Map). The shapefile for the dry shelves is modified according to [Willmes \(2015\)](#).

For the mapping of aeolian deposits, the digital geological map of Germany with a scale of 1:200,000 served as a major source ([BGR, 2007](#)). It is more precise than the 1:1,000,000 map and the loess distribution map of [Haase et al. \(2007\)](#), see [Figure 1](#). This dataset contains 55 shapefiles corresponding to the 55 map sheets of the original analogue maps ([Figure 2](#)). These shapefiles cover the area of Germany as well as adjacent regions. As the first step, the entire

Quaternary sediments were exported from the attribute table of each shapefile. In the second step, the aeolian sediments were extracted. Hereinafter, those were subdivided into three major classes: loess and loess derivatives, sandy loess, and dunes and aeolian sand (for a more detailed description of the classification, see [Section 3.2](#) and [Table 1](#)). The resulting shapefiles were merged to obtain coherent datasets.

Generalisation of the data, especially for the detailed loess map, was conducted by using a self-built model ([Figure 3](#)). The model performs an automated aggregation, simplification and smoothing to adjust the obtained data to the smaller scale of the resultant maps. The shapefiles were aggregated three times, whereby different values for the minimum hole size and the minimum area were applied. Therefore, the aggregation algorithm scans the shapefile in order to detect all polygons and holes in the shapefile ([ESRI, 2016a](#)). Shapefiles smaller than 1 km² were deleted and holes smaller than 10 km² were filled. Afterwards, the aggregated shapefile was simplified using a Bend-Simplify Algorithm and smoothed with a PAEK Algorithm ([ESRI, 2016b, 2016c](#); [Regnauld & McMaster, 2007](#)). The specific parameters for all generalisation steps are shown in [Figure 3](#). For both maps, the same generalisation steps were chosen to create a smooth and consistent map design. Since the focus of the study is on Germany, the map contents were clipped with the German national borders, albeit the distribution of the sediments is cross-border.

To allow better orientation, major rivers ([JRC, 2007](#); [Vogt et al., 2007](#)), administrative borders ([gadm.org, 2018](#)) as well as major cities were inserted in the map. Additionally, the 1-arc-second Japan Aerospace Exploration Agency (JAXA) Advanced Land Observing Satellite (ALOS) averaged digital surface model (DSM) was used to extract topographical information ([JAXA EORC, 2016](#)). This globally available elevation model is based on the AW3D dataset, which has a spatial resolution of ~5 m. The high-resolution data were derived from stereographic multi-temporal satellite imaginaries, which were stacked, mosaicked and validated with existing height references such as the data from the Ice, Cloud and land Elevation Satellite (ICESat) mission as well as SRTM version 2 data. This dataset was down-sampled to offer the elevation data free of charge. The resultant DSM has a resolution of ~30 m and a height accuracy of less than 5 m and is downloadable in 1x1 tiles ([Tadono et al., 2014, 2016](#); [Takaku, Tadono, & Tsutsui, 2014](#); [Takaku, Tadono, Tsutsui, & Ichikawa, 2016](#)). These tiles were mosaicked to obtain seamless and accurate elevation data for the study area.

We assume that sedimentological conditions of loess distribution (or dust deposition) and sediment relocation are related to relief conditions ([Lehmkuhl et al., 2016](#)), so a topographical analysis of the aeolian

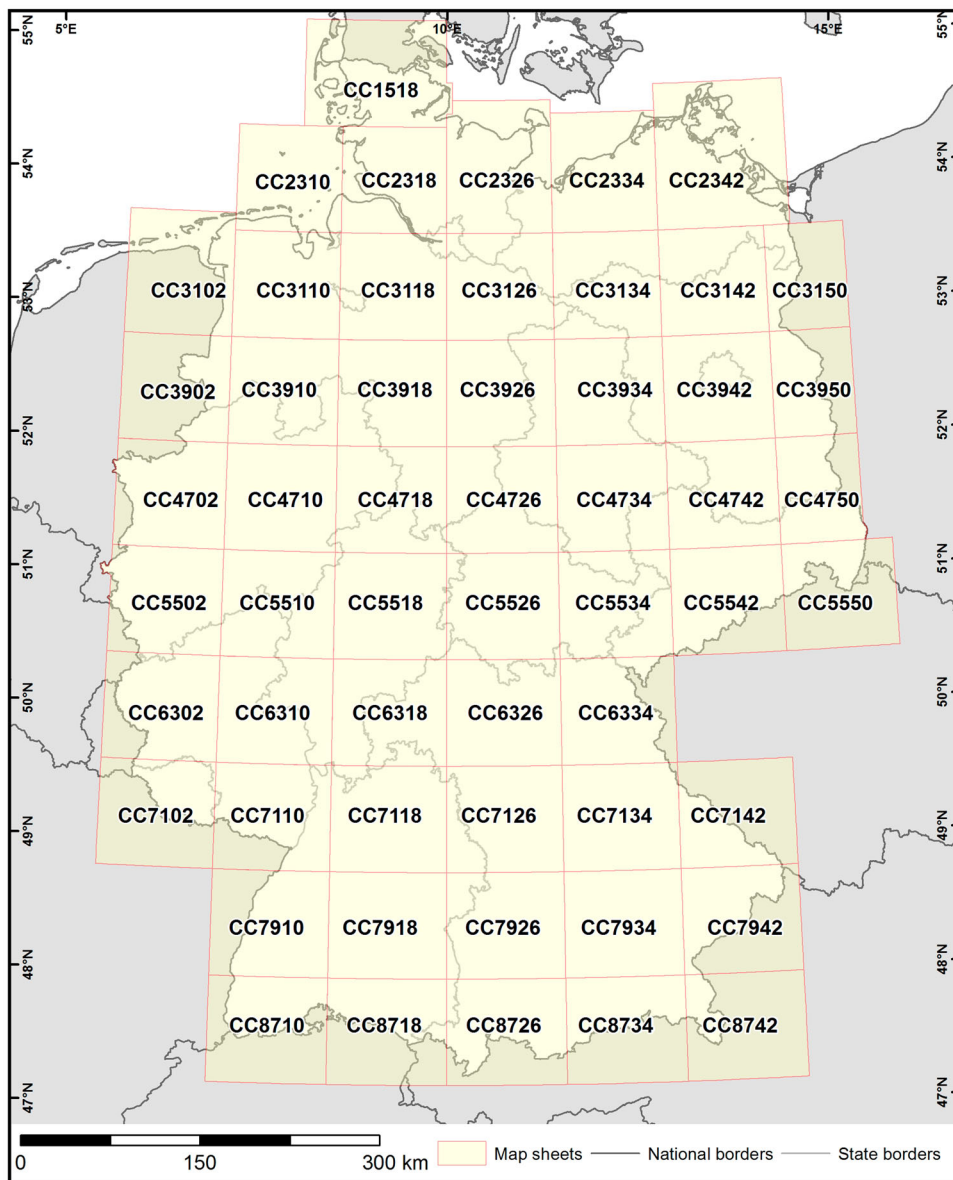


Figure 2. Index map of the German geological map (1:200,000). The designations of the map sheets correspond to nomenclature given by the BGR.

sediments was conducted. The ALOS DSM was clipped with the generalised shapefiles to obtain elevation data for the sediment distribution. The results are shown in Section 4.

The coordinate reference system of the source shapefiles was the Gauß-Krüger-based German Main Triangle Net (Deutsches Hauptdreiecksnetz (DHDN)

Zone 3, EPSG: 31467). In order to create a dataset which can be used internationally, the shapefiles were transformed to the European Terrestrial Reference System (ETRS) 1989 Lambert's Equal Area projection (LAEA; EPSG: 3035), as recommended by the European Union (INSPIRE, 2014).

3.2. Differences in mapping and loess definitions

The definitions of and the clear distinction between loess, loess-like sediments and loess derivatives have been disputed for several decades (Pécsi & Richter, 1996; Pye, 1995; Smalley et al., 2001; Sprafke & Obreht, 2016). These discrepancies hamper a simple mapping of said sediments. The problems occurring from cross-border mapping can be seen, e.g. in the loess distribution map of Haase et al. (2007), where in some cases administrative borders correspond to the

Table 1. Combined classes of aeolian sediments used in the final map.

Original maps	Resultant map
Loess	Loess and loess derivatives
Loess loam	
Loess and loess loam	
Sandy loess	Sandy loess
Flottsand	
Dunes	Dunes and aeolian sands
Aeolian sand	
Dunes and aeolian sand	

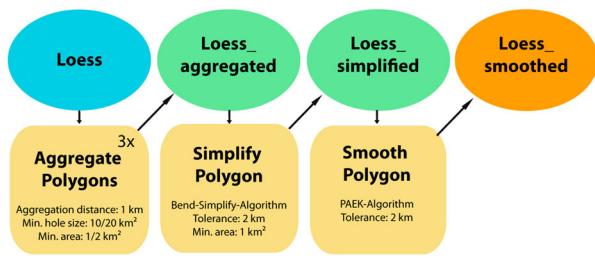


Figure 3. Generalisation model built in ArcMap 10.4.1. The figure shows the model scheme for the loess and loess derivatives shapefile ('Loess') as an example. The blue ellipse represents the original data, the green ellipses intermediate results and the orange ellipse the resultant shapefile. The squares represent the applied tools with specific tool parameters. Note that polygon aggregation was performed three times in order to eliminate small areas and gaps within the shapefiles.

boundaries of loess distribution. An approach to overcome these cross-border issues, e.g. using geological and paedological data is given in Lindner et al. (2017).

In Germany, the mapping of loess and loess derivatives started at the end of the nineteenth century and was mainly conducted by the Prussian Geological Survey (Preußische Geologische Landesanstalt, Wagenbreth, 1999). In the course of these mappings, only sediments with a thickness of more than 2 m were taken into account. This led to gaps, especially concerning the loess distribution. Additional problems

occur because of federalism; each of the 16 federal states in Germany maintains its own geological survey. Thematic maps encompassing several administrative entities tend to show artificial breaks, e.g. at administrative borders (cf. Nilson, Köthe, & Lehmkühl, 2007, and references therein). The 16 geological surveys compiled the 55 maps, based on a multitude of source data. These surveys spread over a time span of more than 30 years and were conducted by a large number of workers. The maps were digitised and published online in 2007. In this step, the data were not homogenised, leading to the variety of aeolian sediment classes. In some cases, even two maps of the same geological survey can show distinctive differences regarding the mapping or nomenclature (Figure 4). In order to simplify and synthesise the different maps, several classes were combined (Table 1).

The nomenclature of the source deposits is even more diverse. For example, the Munich gravel plain (see Section 4.4) is designated as 'lower terrace' as well as 'Würmian fluvial sediments' in two adjacent map sheets of the same geological survey (Figure 4). To avoid false mapping results, these sediments were extracted from source data with a smaller scale, which was the geological map at 1:1,000,000 scale (see Section 3.1).

Only sediments of primary aeolian origin were included. Sediments which were significantly altered such as by weathering (German: Verwitterungsbildungen)

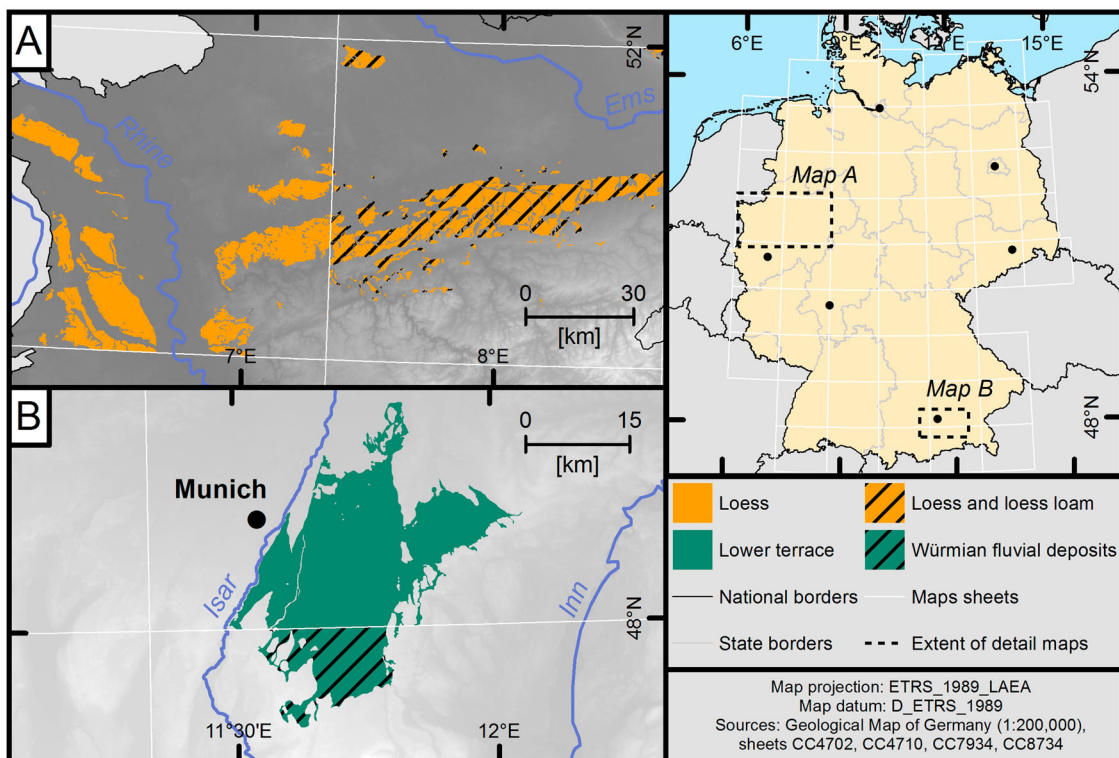


Figure 4. Two examples of different mapping at borders between adjacent map sheets. Map A shows aeolian sediments in western Germany. Only loess and loess-like sediments were considered. Map B shows the differences of fluvial sediments in southern Germany. Only the fluvial sediments east of the Isar River are shown to underline the differences in mapping within one sediment body. This artificial break between the different maps can be found throughout the study area.

or redeposition (German: Umlagerungsbildungen) were not taken into account, even though their primary origin could be aeolian. For information about the spatial distribution of relocated or colluviated loess, see [Bertran et al. \(2016\)](#).

The resultant map of the aeolian sediments is compared to two existing maps: the map of [Haase et al. \(2007\)](#) as the widely accepted reference and the map of [Bertran et al. \(2016\)](#) as a recent work with an approach differing from ours.

4. Distribution of loess and aeolian sediments in Germany

The following section focuses on the presentation and discussion of our results. The distribution of aeolian sediments is described for the different regions in connection with the potential source areas.

4.1. Aeolian and fluvio-glacial sediments in northern Germany

Especially in map A we show the distribution of alluvial fill, the lower terrace, the fluvio-glacial valleys (Urstromtäler) and the Weichselian fluvio-glacial deposits. The latter comprise mainly sandar (glacio-fluvial outlet plains) which correspond to the different extents of the late Pleistocene ice sheet. Some of these glacio-fluvial outlet plains are related to the retreat of the Weichselian ice sheet (Frankfurt and Pommerian stages) and are, therefore, located further to the northeast than the maximum ice marginal position. We added these selected late Pleistocene sediments, as they represent a major local dust source.

4.2. The Northern Central European loess belt including sandy loess

Map B (Main Map) shows the belt-shaped distribution of loess on the northern margin of the German uplands (LR1). This pattern is almost parallel to potential source areas – especially the glacio-fluvial deposits and the Urstromtäler – in northeast Germany. Grain size decreases with increasing distance from the Fennoscandia Ice sheet, especially in the eastern part of Germany: aeolian sand and sandy loess (in some areas and maps named Flottsand in German) can be found in proximity to the source areas (e.g. east of Hamburg respectively south of Berlin), whereas loess and its derivatives can be found in distal positions. The North Sea was a vast outwash plain during the LGM and act as additional major particle source. It is noticeable that there are aeolian sand covers beneath the ice sheet of the LGM. These sediments were probably deposited during the late Weichselian or even during the Holocene after ice retreat ([Hilgers, Murray, Schlaak, & Radtke, 2001](#); [Koster, 2005](#); [Küster &](#)

[Preusser, 2010](#)). Sandy loess is only present in elevations lower than 200 m a.s.l. ([Figure 5](#)). Most loess in this region is distributed in front of the German mountain ranges in lower elevations. This topographic barrier limits loess distribution to elevations roughly between 190 and 390 m a.s.l. The sand belt north of the loess region as represented by [Zeeberg \(1998\)](#) and [Bertran et al. \(2016\)](#) shows that the loess is juxtaposed to sand. In our map, the coversands are poorly represented as the uppermost 2 m were not included in the geological mapping.

4.3. The Upper Rhine Valley including the Mainz basin

Principal accumulation areas of loess in the Upper Rhine Valley are the rift flanks of the Upper Rhine graben. It should be noted that the loess distribution on the west bank of the Rhine is more distinctive than its eastern counterpart. The deposits in the west extend across the graben, whereas the loess in the east can be found at the margin of the Black Forest. The northeastern Upper Rhine valley is dominated by aeolian cover sands, which merge into the broad sand covers in the area of Frankfurt am Main. The sand material originated from the Pleistocene braided Rhine River. Elevations, especially in the Mainz basin north of the valley, exceed those in northern Germany (see LR2 in [Figure 5](#)). Another peculiarity of this region is the direct vicinity of loess deposits and their potential source areas. Southeast of Frankfurt am Main, triangular-shaped loess deposits are interposed with late Pleistocene fluvial deposits of the Rhine.

4.4. The basins of the German uplands

The third mentioned loess region are the basins within the German uplands. Due to the topographic limitation of these basins, the distribution pattern of their deposits is rather fragmentary. Exceptions are the broad basins in western Franconia (3b) and the Kraichgau (3a), southeast respectively south of Frankfurt am Main. The loess distribution spreads over elevations of 250–600 m a.s.l. (LR3 in [Figure 5](#)), with some outliers at both the upper and lower ranges.

4.5. Loess along the Danube

The loess distribution related to the Danube stretches along the upper reaches of the river. They can be mainly found between the Danube River in the north and the Würmian ice margin in the south. Akin to the Upper Rhine Valley, the sediments can be found directly next to the fluvial source areas. As a peculiarity, the Munich gravel plain – a Pleistocene fluvial sediment body with an area of $\sim 1300 \text{ km}^2$ – has to be mentioned. The topographical distribution of the Danube

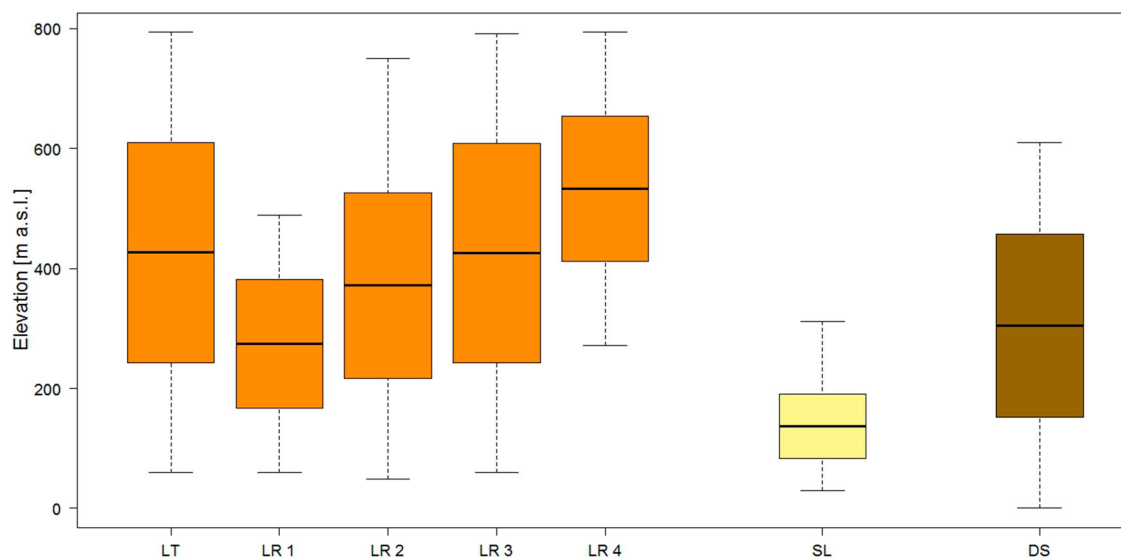


Figure 5. Boxplots showing the elevational distribution of the aeolian sediments in Germany (LT: loess total, LR1–4: loess regions 1–4, SL: sandy loess, DS: dunes and aeolian sands). Designations of the loess regions in accordance to Figure 1.

loess in Germany shows the highest elevations, ranging between 400 and 650 m a.s.l., with a maximum of almost 800 m (LR4 in Figure 5).

5. Discussion

The datasets used and the methods applied must be discussed critically. The discrepancies in loess mapping mentioned in Section 3.2 limit the possibility to differentiate between various loess facies. In our map, loess and its derivatives, which are given in more detail in the geological maps, were combined to one class. There is no possibility to differentiate between loess and loess loam for example. Prima facie, this may appear as a loss of information. As there are various definitions of loess, loess derivatives, and loess-like sediments, sharp boundaries between those facies, as they are often presented in maps, feign high accuracies, which cannot be given at this scale. Such detailed distinctions cannot be extracted from geological maps, but should be investigated in selective (field) case studies.

Thus, the resolution is strongly dependent on generalisation. The model used was created in an iterative procedure, in which the intermediate products were evaluated thoroughly. Table 2 shows that the general area of the mapped sediments increased. These enlargements can be easily explained by the aggregation of small polygons. These were found in hilly areas with a distinctive surface geology. In the original map, all geological structures were taken into account. This leads to the fragmented visual appearance that is not suitable for a map of such a small scale. Due to the focus of our map on the aeolian sediments, those expansions were accepted to obtain a coherent design. The expansion of the polygons cannot only be seen in the increased total area, but also in the growth of the averaged polygon size. The values are an order of magnitude higher than the polygons of the original map, albeit most of them are smaller than the ones in the map of Haase et al. (2007), indicating a higher resolution (Table 2). The distribution of aeolian sediments between the maps seems comparable, although our map's generalisation is smoother and shows less loss

Table 2. Comparison of the polygon areas between the raw data from the geological maps, the resultant map and the datasets published by Haase et al. (2007) and Bertran et al. (2016).

	Geological map		Resultant map		Haase et al. (2007)		Bertran et al. (2016)	
	Area (km ²)	Mean (km ²)	Area (km ²)	Mean (km ²)	Area (km ²)	Mean (km ²)	Area (km ²)	Mean (km ²)
LT	29,841	2	40,720	54	55,429	122	29,974	8
LR1	14,514	3	19,571	202	30,357	112	22,111	17
LR2	1853	2	2717	53	2682	108	908	5
LR3	6580	2	11,494	52	10,993	107	5505	4
LR4	3825	2	6067	58	9538	191	1190	2
CL	–	–	–	–	–	–	25,833	6
SL	2068	4	2372	36	5085	116	–	–
SS	–	–	–	–	–	–	11,023	10
DS	10,123	1	14,290	20	5728	110	77,971	50

Note: Area refers to the total area of the sediments (for abbreviations, see Figure 5; CL: colluviated loess, SS: silty sand), mean refers to the averaged size of the polygons of each shapefile.

of information. This can be seen in smaller mean values of the size of polygons as well as in the overestimation of widespread loess regions in the Haase map (LR1 and LR4).

The comparison to the map published by [Bertran et al. \(2016\)](#) shows significant similarities and some differences: The mean areas are much smaller than in our map, resulting from raster source data with a resolution of 500×500 m. The loess distribution in LR1, 2 and 3 match, albeit there are regional differences such as in Saxony and south of the Harz Mountains. LR1 shows a particular high concordance in pattern and area. Larger discrepancies can be seen in LR4, where our map shows widespread loess deposits, whereas the [Bertran et al. \(2016\)](#) map shows only fragmentary patches. Those differences can be explained by the mapping of relocated and colluviated loess in this map, leading to an underrepresentation of loess and loess derivatives. Accordingly, a large proportion of LR4 loess are mapped as loess derivatives by [Haase et al. \(2007\)](#) and as colluviated loess by [Bertran et al. \(2016\)](#). Although sandy loess was not considered, silty sand is mapped as a transitional facies between sand and loess. The aeolian sand in northern Germany in the map of [Bertran et al. \(2016\)](#) shows the most striking differences to ours: while our map shows fragmentary distribution of sand, [Bertran et al. \(2016\)](#) mapped wide areas, whereas other aeolian sand deposits, such as in the area of Frankfurt am Main, are not included. This may be either an overestimation by [Bertran et al. \(2016\)](#) or more likely an underestimation in our map, since only sand deposits with a specific thickness were mapped, which are not always reached in northern Germany. As mapped by [Zeeberg \(1998\)](#) and [Bertran et al. \(2016\)](#), the coversands form an almost continuous band juxtaposed to the loess, which better highlight the grain-size gradient in the aeolian deposits.

6. Conclusions

This study provides detailed maps of the distribution of aeolian sediments and their potential source areas in Germany. The use of freely available geological data simplified the data provision, but is accompanied by some impediments:

- The focus of geological mapping usually does not lie on the Quaternary deposits, which leads to a fragmentation of the sediment distribution in maps.
- This method does not allow any assertions about the thickness or detailed timing of deposition of the sediments. There is no nationwide information about the mapping procedure, so we cannot state whether, for example, the uppermost 2 m was included into the geological mapping. Therefore, the sediment thickness cannot be determined precisely.

- The geological mapping spanned a long period of time and includes a multitude of different mappers. Due to the various procedures and loess definitions, artificial boundaries occur not just at administrative borders, but also within the same map sheet.

Here, we tried to overcome these issues by creating a seamless, coherent dataset. In order to achieve that aim, we propose the following solutions:

- The extraction and generalisation of the shapefiles place the focus on aeolian sediments. Especially the generalisation eliminates the fragmentary pattern of the shapefiles. However, this must be taken into account, when discussing the data. The comparison to existing datasets is crucial to validate our map: the comparison to the map of [Haase et al. \(2007\)](#) shows that our map experienced an appropriate degree of generalisation. This leads to a high accuracy combined with good readability on a small scale. Compared to the map of [Bertran et al. \(2016\)](#), we see similarities in loess distribution, whereas the aeolian sand deposits in Germany in this map require further validation.
- The thickness of a sedimentary body is indeed important information. Across a broad study area like Germany, information about the thickness feign a degree of accuracy, which cannot be given on this scale. Therefore, this issue could not be solved by our study.
- Even though the distinction between different loess facies is not possible within our map, it provides an overview of the distribution of aeolian sediments. However, a more detailed approach is not possible on such a scale and should be provided by regional (field) case studies.

Thus, the map presents the geographical distribution of aeolian sediments within regional clusters, which are characterised by different topographical situations. The distribution of loess shows an increasing elevation southwards and also sandy loess displays a characteristic elevation below 200 m. The map indicates that geomorphological features like mountain ranges, valleys and graben structures variously act as barriers or sinks for loess accumulation. These features and the distribution of the aeolian sediments as well as their potential source areas allow conclusions about the palaeogeographical conditions in Germany. Our work highlights the value of the compiled geodata, which can be accessed freely at the CRC806 database at <http://dx.doi.org/10.5880/SFB806.39>.

Software

Mapping, processing and statistical analysis were done using ESRI ArcGIS 10.4.1 in focus of reproducibility

and the broad availability of this software. Statistics were analysed using R 3.4.1 (R Core Team, 2014) and Microsoft Excel 2013. Main graphics were created using R 3.4.1 or Adobe Illustrator.

Acknowledgements

We thank D. Haase for sharing shapefiles of the loess distribution map and P. Bertran for providing the shapefiles of the distribution of aeolian sediments modelled by his team. S. Vlamincx helped with comments on the manuscript. The BGR is thanked for the provision of the geological data. In addition, we would like to thank the reviewers P. Bertran, S.B. Marković and C. Orton and the associate editor J. Knight for helpful suggestions to improve the map and paper.


Disclosure statement

No potential conflict of interest was reported by the authors.

Funding

The investigations were carried out in the frame of the CRC 806 ‘Our way to Europe’, subproject D1 ‘Analysis of Migration Processes due to Environmental Conditions between 40,000 and 14,000 a BP in the Rhine Catchment and Adjacent Areas’, supported by the DFG (Deutsche Forschungsgemeinschaft, Grant number INST 216/596-3).

ORCID

Frank Lehmkuhl  <http://orcid.org/0000-0002-6876-7377>
Stephan Pötter  <http://orcid.org/0000-0003-0059-5270>
Janina Böskén  <http://orcid.org/0000-0001-8431-0484>

References

- Antoine, P., Catt, J., Lautridou, J.-P., & Sommé, J. (2003). The loess and coversands of northern France and southern England. *Journal of Quaternary Science*, 18(3–4), 309–318. doi:10.1002/jqs.750
- Antoine, P., Rousseau, D.-D., Degeai, J.-P., Moine, O., Lagroix, F., Kreuzer, S., ... Lisá, L. (2013). High-resolution record of the environmental response to climatic variations during the last interglacial–glacial cycle in central Europe: The loess–palaeosol sequence of Dolní Věstonice (Czech Republic). *Quaternary Science Reviews*, 67, 17–38. doi:10.1016/j.quascirev.2013.01.014
- Bertran, P., Liard, M., Sitzia, L., & Tissoux, H. (2016). A map of Pleistocene aeolian deposits in western Europe, with special emphasis on France. *Journal of Quaternary Science*, 31(8), e2909. doi:10.1002/jqs.2909
- BGR. (2007). *Geologische Übersichtskarte der Bundesrepublik Deutschland 1:200.000 (GÜK200) - Datenserie*. Retrieved from https://produktcenter.bgr.de/terraCatalog/Query/Detail.do?fileIdentifier=ABA9633F-E0BA-438D-918C-6B3BEB4D641C&pageId=brief_BROWSER_QUERY_FRAME&history=catalogHistory
- Catt, J. A. (1988). *Quaternary geology for scientists and engineers*. Chichester: E. Horwood. Distributed by Halsted Press.
- Catt, J. A. (2001). The agricultural importance of loess. *Earth-Science Reviews*, 54(1–3), 213–229. doi:10.1016/S0012-8252(01)00049-6.
- Ehlers, J., Eissmann, L., Lippstreu, L., Stephan, H.-J., & Wansa, S. (2004). Pleistocene glaciations of north Germany. In *Developments in quaternary sciences* (Vol. 2, pp. 135–146). Elsevier. doi:10.1016/S1571-0866(04)80064-2
- Ehlers, J., Grube, A., Stephan, H.-J., & Wansa, S. (2011). Pleistocene glaciations of north Germany – new results. In *Developments in quaternary sciences* (Vol. 15, pp. 149–162). Elsevier. doi:10.1016/B978-0-444-53447-7.00013-1
- Einwögerer, T., Friesinger, H., Händel, M., Neugebauer-Maresch, C., Simon, U., & Teschler-Nicola, M. (2006). Upper palaeolithic infant burials. *Nature*, 444(7117), 285–285. doi:10.1038/444285a
- ESRI. (2016a). *Aggregate polygons*. Retrieved from <http://desktop.arcgis.com/en/arcmap/10.3/tools/cartography-toolbox/aggregate-polygons.htm>
- ESRI. (2016b). *Simplify polygon*. Retrieved from <http://desktop.arcgis.com/en/arcmap/10.3/tools/cartography-toolbox/simplify-polygon.htm>
- ESRI. (2016c). *Smooth polygon*. Retrieved from <http://desktop.arcgis.com/en/arcmap/10.3/tools/cartography-toolbox/smooth-polygon.htm>
- Fink, J., Haase, G., & Ruske, R. (1977). Bemerkung zur Lösskarte von Europa 1:2,5 Mio. *Petermanns Geographische Mitteilungen*, 2(77), 81–97.
- Flint, R. F. (1971). *Glacial and quaternary geology*. New York, NY: Wiley.
- gadm.org. (2018). *Global administrative areas – boundaries without limits*. Retrieved from <http://gadm.org/>
- Gerlach, R., Baumewerd-Schmidt, H., van den Borg, K., Eckmeier, E., & Schmidt, M. W. I. (2006). Prehistoric alteration of soil in the Lower Rhine Basin, northwest Germany – archaeological, ¹⁴C and geochemical evidence. *Geoderma*, 136(1–2), 38–50. doi:10.1016/j.geoderma.2006.01.011
- Grahmann, R. (1932). *Der Löss in Europa* (Vol. 51). Leipzig: Duncker & Humblot.
- Haase, D., Fink, J., Haase, G., Ruske, R., Pécsi, M., Richter, H., ... Jäger, K.-D. (2007). Loess in Europe – Its spatial distribution based on a European Loess Map, scale 1:2,500,000. *Quaternary Science Reviews*, 26(9–10), 1301–1312. doi:10.1016/j.quascirev.2007.02.003
- Händel, M., Simon, U., Einwögerer, T., & Neugebauer-Maresch, C. (2009). Loess deposits and the conservation of the archaeological record – The Krems-Wachtberg example. *Quaternary International*, 198(1–2), 46–50. doi:10.1016/j.quaint.2008.07.005
- Hilgers, A., Murray, A., Schlaak, N., & Radtke, U. (2001). Comparison of quartz OSL protocols using lateglacial and Holocene dune sands from Brandenburg, Germany. *Quaternary Science Reviews*, 20(5–9), 731–736. doi:10.1016/S0277-3791(00)00050-0
- INSPIRE. (2014). *D2.8.I.1 Data Specification on Coordinate Reference Systems - Technical Guidelines*. Brussels: INSPIRE Thematic Working Group Coordinate Reference Systems & Geographical Grid Systems.
- JAXA EORC. (2016). *ALOS global digital surface model “ALOS World 3D - 30m” (AW3D30)*. Retrieved from <http://www.eorc.jaxa.jp/ALOS/en/aw3d30/index.htm>
- JRC. (2007). *Catchment characterisation and modelling*. Retrieved from <http://ccm.jrc.ec.europa.eu/php/index.php?action=view&id=23>
- Koster, E. A. (2005). Recent advances in luminescence dating of Late Pleistocene (cold-climate) aeolian sand and loess

- deposits in western Europe. *Permafrost and Periglacial Processes*, 16(1), 131–143. doi:10.1002/ppp.512
- Küster, M., & Preusser, F. (2010). Late glacial and Holocene aeolian sands and soil formation from the Pomeranian outwash plain (Mecklenburg, NE-Germany). *E&G Quaternary Science Journal*, 58, 156–163. doi:10.3285/eg.58.2.04
- Lehmkuhl, F., Zens, J., Krauß, L., Schulte, P., & Kels, H. (2016). Loess-paleosol sequences at the northern European loess belt in Germany: Distribution, geomorphology and stratigraphy. *Quaternary Science Reviews*, 153, 11–30. doi:10.1016/j.quascirev.2016.10.008
- Liedtke, H., & Marcinek, J. (Eds.). (2002). *Physische Geographie Deutschlands: 84 Tabellen* (3., überarb. und erw. Aufl). Gotha: Klett-Perthes.
- Lill, G. O., & Smalley, I. J. (1978). Distribution of loess in Britain. *Proceedings of the Geologists' Association*, 89(1), 57–65. doi:10.1016/S0016-7878(78)80021-2
- Lindner, H., Lehmkuhl, F., & Zeeden, C. (2017). Spatial loess distribution in the eastern Carpathian Basin: A novel approach based on geoscientific maps and data. *Journal of Maps*, 13(2), 173–181. doi:10.1080/17445647.2017.1279083
- Marković, S. B., Stevens, T., Kukla, G. J., Hambach, U., Fitzsimmons, K. E., Gibbard, P., ... Svirčev, Z. (2015). Danube loess stratigraphy — Towards a pan-European loess stratigraphic model. *Earth-Science Reviews*, 148, 228–258. doi:10.1016/j.earscirev.2015.06.005
- Muhs, D. R., & Bettis, E. A. (2003). Quaternary loess-Paleosol sequences as examples of climate-driven sedimentary extremes. In *Extreme depositional environments: Mega end members in geologic time* (Vol. 370, pp. 53–74). Geological Society of America. doi:10.1130/0-8137-2370-1.53
- Neugebauer-Maresch, C., Einwögerer, T., Richter, J., Maier, A., & Hussain, S. T. (2016). Kammern-Grubgraben. Neue Erkenntnisse zu den Grabungen 1985–1994. *Archaeologia Austriaca*, 1, 225–254. doi:10.1553/archaeologia100s225
- Nilson, E., Köthe, R., & Lehmkuhl, F. (2007). Categorising inconsistencies between national GIS data in Central Europe: Case studies from the country triangle of Belgium, the Netherlands and Germany. *Applied GIS*, 3, 1–20.
- Orgiazzi, A., Ballabio, C., Panagos, P., Jones, A., & Fernández-Ugalde, O. (2018). LUCAS soil, the largest expandable soil dataset for Europe: A review: LUCAS soil, pan-European open-access soil dataset. *European Journal of Soil Science*, 69(1), 140–153. doi:10.1111/ejss.12499
- Pécsi, M. (1990). Loess is not just the accumulation of dust. *Quaternary International*, 7, 1–21.
- Pécsi, M. (1991). Problems of loess chronology. *GeoJournal*, 24(2), 143–150. doi:10.1007/BF00186009
- Pécsi, M., & Richter, G. (1996). Loess - Herkunft - Gliederung - Landschaften. *Zeitschrift für Geomorphologie, Supplementary Issues*, 98, 1–391.
- Pye, K. (1995). The nature, origin and accumulation of loess. *Quaternary Science Reviews*, 14(7–8), 653–667. doi:10.1016/0277-3791(95)00047-X
- R Core Team. (2014). *R: A language and environment for statistical computing*. Vienna: Austria. Retrieved from <http://www.R-project.org>
- Regnaud, N., & McMaster, R. B. (2007). A synoptic view of generalisation operators. In W. Mackaness, A. Ruas, & L. T. Sarjakoski (Eds.), *Generalisation of geographic information* (pp. 37–66). Elsevier. doi:10.1016/B978-008045374-3/50005-3
- Rensink, E. (2010). *Eyserheide: A Magdalenian open-air site in the loess area of the Netherlands and its archaeological context*. Leiden: Leiden University.
- Smalley, I., Marković, S. B., & Svirčev, Z. (2011). Loess is [almost totally formed by] the accumulation of dust. *Quaternary International*, 240(1–2), 4–11. doi:10.1016/j.quaint.2010.07.011
- Smalley, I., O'Hara-Dhand, K., Wint, J., Machalett, B., Jary, Z., & Jefferson, I. (2009). Rivers and loess: The significance of long river transportation in the complex event-sequence approach to loess deposit formation. *Quaternary International*, 198(1–2), 7–18. doi:10.1016/j.quaint.2008.06.009
- Smalley, I. J., Jefferson, I. F., Dijkstra, T. A., & Derbyshire, E. (2001). Some major events in the development of the scientific study of loess. *Earth-Science Reviews*, 54(1), 5–18. doi:10.1016/S0012-8252(01)00038-1
- Sprafke, T., & Obrecht, I. (2016). Loess: Rock, sediment or soil – What is missing for its definition? *Quaternary International*, 399, 198–207. doi:10.1016/j.quaint.2015.03.033
- Tadono, T., Ishida, H., Oda, F., Naito, S., Minakawa, K., & Iwamoto, H. (2014). Precise global DEM generation by ALOS PRISM. *ISPRS Annals of Photogrammetry, Remote Sensing and Spatial Information Sciences, II-4*, 71–76. doi:10.5194/isprsannals-II-4-71-2014
- Tadono, T., Nagai, H., Ishida, H., Oda, F., Naito, S., Minakawa, K., & Iwamoto, H. (2016). Generation of the 30 m-mesh global digital surface model by ALOS PRISM. *ISPRS - International Archives of the Photogrammetry, Remote Sensing and Spatial Information Sciences, XLI-B4*, 157–162. doi:10.5194/isprsarchives-XLI-B4-157-2016
- Takaku, J., Tadono, T., & Tsutsui, K. (2014). Generation of high resolution global DSM from ALOS PRISM. *ISPRS - International Archives of the Photogrammetry, Remote Sensing and Spatial Information Sciences, XL-4*, 243–248. doi:10.5194/isprsarchives-XL-4-243-2014
- Takaku, J., Tadono, T., Tsutsui, K., & Ichikawa, M. (2016). Validation of “AW3D” global DSM generated from ALOS PRISM. *ISPRS Annals of Photogrammetry, Remote Sensing and Spatial Information Sciences, III-4*, 25–31. doi:10.5194/isprsannals-III-4-25-2016
- Tasić, N. N., Penezić, K., Marković, S. B., & Catto, N. (2017). Vinča – Garden of Eden. *Quaternary International*, 429, 1–2. doi:10.1016/j.quaint.2017.02.023
- Terhorst, B., Kühn, P., Damm, B., Hambach, U., Meyer-Heintze, S., & Sedov, S. (2013). Paleoenvironmental fluctuations as recorded in the loess-paleosol sequence of the upper paleolithic site Krems-Wachtberg. *Quaternary International*, 351, 67–82. doi:10.1016/j.quaint.2013.03.045
- Toloczyki, M., Trurnit, P., Voges, A., Wittekind, H., & Zitzmann, A. (2006). *Geologische Karte der Bundesrepublik Deutschland 1:1.000.000 (GK1000)*. Hannover: Bundesanstalt für Geowissenschaften und Rohstoffe.
- Tóth, G., Jones, A., Montanarella, L., European Commission, Joint Research Centre, & Institute for Environment and Sustainability. (2013). *LUCAS topsoil survey: Methodology, data and results*. Luxembourg: Publications Office. Retrieved from <http://dx.publications.europa.eu/10.2788/97922>
- Vogt, J., Soille, P., de Jager, A., Rimaviciute, E., Mehl, W., Foisneau, S., ... Bamps, C. (2007). *A pan-European river and catchment database*. Luxembourg: Office for Official Publications of the EC.

Wagenbreth, O. (1999). *Geschichte der Geologie in Deutschland*. Berlin: Springer. doi:10.1007/978-3-662-44712-3

Willmes, C. (2015). LGM sealevel change (HiRes), CRC806 database, Collaborative Research Centre 806. Dataset, Cologne: CRC806 database, Collaborative Research

Centre 806. Retrieved from <http://crc806db.uni-koeln.de/dataset/show/lgm-sealevel-change-hires1436532921>

Zeeberg, J. (1998). The European sand belt in eastern Europe – And comparison of late glacial dune orientation with GCM simulation results. *Boreas*, 28 (2), 127–139. doi:10.1111/j.1502-3885.1998.tb00873.x